ResearchGate

See discussions, stats, and author profiles for this publication at: https://www.researchgate.net/publication/216290847

# Wax precipitation from North Sea crude oils. 3. Pricipitation and dissolution of wax studied by differential scanning calorimetry

**ARTICLE** *in* ENERGY & FUELS · JANUARY 1991

Impact Factor: 2.79

CITATIONS
9

READS
25

**5 AUTHORS**, INCLUDING:

Hans Petter Rønningsen
Statoil ASA
**17** PUBLICATIONS **631** CITATIONS

SEE PROFILE

Available from: Asger B Hansen
Retrieved on: 03 February 2016

*Energy & Fuels* 1991, 5, 914-923

# Wax Precipitation from North Sea Crude Oils. 3. Precipitation and Dissolution of Wax Studied by Differential Scanning Calorimetry

Asger B. Hansen,* Elfinn Larsen, Walther B. Pedersen, and Anne B. Nielsen

*Risø National Laboratory, DK-4000 Roskilde, Denmark*

Hans Petter Rønningsen

*STATOIL a.s., Forus, N-4001 Stavanger, Norway*

*Received April 29, 1991*

Differential scanning calorimetry was used to study wax precipitation from a series of North Sea crude oils by measuring glass transition temperatures, wax precipitation and dissolution temperatures (wax *appearance* and *disappearance*, respectively), and wax precipitation and dissolution enthalpies in the temperature range from +70 to -140 °C. With respect to physical characteristics, the oils ranged from very light paraffinic condensates to heavy waxy crudes including biodegraded and asphaltenic oils. On the basis of glass transition temperatures, the oils could be sorted into groups that corresponded to their physical descriptions, whereas a similar grouping according to the precipitation or dissolution temperatures did not correspond to the physical characteristics. Glass transition temperatures ranged from -128.5 to -81.5 °C, while wax precipitation and dissolution temperatures ranged from +39.5 to -26.0 °C and -16.0 to +53.5 °C, respectively. Dissolution temperatures were generally higher than corresponding precipitation temperatures, 13 °C on the average, and nonequilibrium conditions caused by undercooling and overheating during temperature scanning were probably responsible for these temperature differences. Measured precipitation and dissolution enthalpies based on total sample amounts ranged from 0.55 to 9.79 cal/g and 0.32 to 10.63 cal/g, respectively. On the average, dissolution enthalpies were ca. 14% greater than the corresponding precipitation enthalpies; this excess of enthalpy required for dissolution of wax cannot be accounted for thermodynamically and is supposed to be related to exothermal effects taking place during heating scans and hence the way data are processed. By combining the amount of wax precipitated by cooling from +45 to -40 °C, as determined by pulsed NMR, with the accumulated enthalpy of the same temperature interval, it was possible to express the *average* precipitation and dissolution enthalpies based on the actual amount of wax; values ranged from 23.7 to 70.6 cal/g and from 32.3 to 71.7 cal/g for the precipitation and dissolution enthalpies, respectively. Furthermore, by combining the incremental amount of wax precipitated as function of temperature in 5 °C intervals from +45 to -40 °C, as determined by pulsed NMR, with the incremental wax enthalpies accumulated in the same temperature intervals, an almost reversed parabolic dependency of wax precipitation and dissolution enthalpies on temperature was revealed; the maxima were about -20 °C.

## Introduction

In this series of four papers (parts 1-4) we are summarizing experimental work and the development of an improved thermodynamic model on wax precipitation from crude oils.[1-3] Crude oils are generally very complex chemical systems containing from hundreds to thousands of individual components in the range from simple low molecular weight *n*-alkanes to high molecular weight waxes and asphaltenes. Due to the content of these high molecular weight substances, crude oils are somewhat colloidal in nature.[4] Reservoir crude oils are very close to thermodynamic equilibrium, but during production, changes of pressure and temperature cause a disturbance of the equilibrium and phase separations like liberation of gas, and precipitation of asphaltenes and wax may result.[5] Especially at subambient conditions, wax precipitation can deteriorate flow properties and cause severe problems by plugging valves and flow lines. Two types of wax are commonly encountered in crude oils, i.e., *macrocrystalline* waxes composed of mainly straight-chain paraffins (*n*-alkanes) with varying chain length (about $C_{20}$ to $C_{50}$) and *microcrystalline* or *amorphous* waxes also containing a high proportion of isoparaffins and naphthenes (cyclic alkanes) with somewhat higher carbon numbers ($C_{30}$ to $C_{60}$);[6] these two types of wax have different properties regarding crystal growth and morphology.[7] [Note: *wax* is used as a general term throughout the text to describe all kinds of solid matter being precipitated or dissolved during cooling and heating whenever no special reference is made to macrocrystalline wax, microcrystalline wax, amorphous wax, etc.] Wax (high molecular weight) precipitation, which basically is a result of a decreased carrying capacity of the fluid solvent (low molecular weight), commences when the crude oil is cooled below its cloud point.

* To whom correspondence should be addressed.

(1) Rønningsen, H. P.; Bjørndal, B.; Hansen, A. B.; Pedersen, W. B. *Energy Fuels*, this issue.
(2) Pedersen, W. B.; Hansen, A. B.; Larsen, E.; Nielsen, A. B.; Rønningsen, H. P. *Energy Fuels*, this issue.
(3) Pedersen, K. S.; Skovborg, P.; Rønningsen, H. P. *Energy Fuels*, this issue.
(4) Dwiggins Jr., C. W. *J. Appl. Crystallogr.* **1978**, *11*, 615-619.
(5) Carnahan, N. F. *J. Pet. Technol.* **1989**, 1024-1025, 1106.
(6) Mazee, W. M. In *Modern Petroleum Technology*, 4th ed.; Hobson, G. D., Pohl, W., Eds.; Applied Science Publishers: Barking, Essex, U.K., 1973; pp 782-803.
(7) Chichakli, M., Jessen, F. W. *Ind. Eng. Chem.* **1967**, *59*, 86-98.

0887-0624/91/2505-0914$02.50/0 © 1991 American Chemical Society

The crystals formed may develop an interlocking 3D structure that can effectively entrap the solvating oil; this will lead to higher viscosity and ultimately gelling and congealing.[5] The temperature at which this happens is known as the pour point, where viscosity and flow properties change dramatically. Even with as little as 2% precipitated wax, gelling may occur.[8] Wax precipitation and low-temperature flow properties of crude oils depend not only on their *n*-paraffin content but also on the oil matrix itself the properties of which aromatics, polar compounds, and asphaltenes can influence significantly.[9]

The present paper deals with the study of thermal effects associated with wax precipitation for a series of crude oils by means of differential scanning calorimetry (DSC). A general description of this technique has been given recently by McNaughton and Mortimer.[10] The thermal analysis of petroleum products in general has been reviewed by Wesolowski,[11] while DSC is particular has been used to characterize and study thermal effects of different types of wax,[12-15] crude oils,[16,17] and other petroleum products.[18-25] More specifically, in a series of papers Bosselet et al.[26-29] studied synthetic oils consisting of *n*-alkanes in dewaxed gas oils to obtain information on the effect of wax composition on crystallization enthalpies and precipitation temperatures; in a similar study of thermal behavior of crude oils, Claudy et al.[16] made attempts to estimate the amount of wax in oils using a derived enthalpy–temperature correlation. In this paper we describe the characterization of 17 North Sea crude oils by DSC in the temperature range of +70 to −140 °C. Apart from two biodegraded oils, oils 1 and 11, these oils range from light paraffinic/waxy condensates (oils 4, 10, 12, 13, and 15) over intermediate paraffinic (oils 2, 7, 8, 16, and 17) to heavier waxy crudes (oils 3, 5, 6, 9, and 14) as described in part 1.[1] For all oils, both the glass transition temperature ($T_g$) and wax precipitation (*appearance*) and dissolution (*disappearance*) temperatures (WPT and WDT) have been studied together with the transition enthalpies involved in the precipitation and dissolution of wax (ideally, heats of *crystallization* and *fusion*), $\Delta H_{wp}$ and $\Delta H_{wd}$, respectively. Furthermore, on the basis of combination of the experimental enthalpy data with the reported pulsed NMR data for the same oils (cf. part 2),[2] the observed enthalpies have been expressed on the basis of the actual amount of wax precipitating from each oil. The combination of pulsed NMR data with DSC data has also been used in an attempt to describe the dependency of the transition enthalpies on temperature.

## Experimental Section

**Apparatus.** All analyses were performed using a Perkin-Elmer System 4 thermal analyzer including the DSC-4 differential scanning calorimeter, a microprocessor controller, an interface, and a PE 3600 data station running under the PETOS operating system. All data acquisition, handling, and analysis was achieved using the Perkin-Elmer TADS thermal analysis software including the special partial area routine. In order to extend the analyses beyond crude oil glass transition temperatures (∼−110 °C), a liquid nitrogen (liq $N_2$) cooling accessory was constructed and built into the DSC-4. This tailor-made all-copper flow cell mounted directly onto the sample holder assembly ascertained that cooling was constant and eliminated the problems with otherwise drifting baselines. During analyses, the sample compartment was constantly flushed with helium (He). Furthermore, to avoid condensation of moisture at the sample holder, a tailor-made Plexiglas glovebox was installed on top of the sample holder and constantly purged with dry $N_2$.

**Sample Preparation and Analysis.** Oil samples to be analyzed were heated to 70 °C in closed containers and shaken thoroughly to ensure complete dissolution of precipitated solids. They were then left to cool to an ambient temperature and shaken again to ensure homogeneity before samples were taken out and transferred to tared sample capsules and weighed. Stainless steel capsules (75 μL) consisting of a pan and a lid with a rubber O-ring were used for both samples and reference (blank). The O-ring sealed the capsule when the bottom and lid were pressed together. The filled and closed sample capsules were heated to 80 °C for 10–15 min to check for leakage and proper assembling by visual inspection before being placed in the DSC-4 sample holder for analysis. This type of stainless steel capsule (Perkin Elmer, part no. 0319-0218) turned out to be superior to both traditional capsules (aluminum) and high-pressure ones with respect to sample volume, tightness, and handling.

All oil samples were analyzed using both cooling and heating temperature programming. Under cooling conditions the DSC-4 was ramped to 70 °C to eliminate any thermal history of the sample and then cooled at a rate of −10 °C/min to −140 °C. In a heating scan the temperature program started at −140 °C directly following the cooling scan and proceeded with a +10 °C/min gradient to 70 °C. All samples were generally analyzed at least five times to improve precision.

**Baseline Adjustment and Calibration.** To ensure that blank thermograms were as flat and horizontal as possible over the entire temperature range of interest, the slope and balance of the instrument were adjusted according to the actual analysis conditions. After proper adjustment, analyses were performed with empty sample and reference capsules to obtain a blank thermogram. This thermogram (*baseline*) was stored in the data station and subtracted from all subsequent sample thermograms during data acquisition to eliminate possible instrument/capsule effects. New baselines were run frequently to compensate for possible instrument drifting.

The DSC-4 instrument was adjusted with respect to both temperature and heat flow using pure indium (In) as a standard. A few micrograms of In (Perkin Elmer, part no. 319-0018; mp 156.60 °C, $\Delta H_f$ 6.80 cal/g) were transferred to the sample capsule and heated above the In melting point to ensure good thermal contact with the sample cup prior to being cooled (−10 °C/min) below its freezing point; the capsule was then heated again (+10 °C/min) and the melting enthalpy (heat of fusion) and the melting point of the sample were recorded. The melting point was defined as the extrapolated peak onset determined by the intersection of the baseline with the inflection line of the peak front (tangent to the *leading edge*). Then the temperature and energy offsets

(8) Krishna, R.; Joshi, G. C.; Purohit, R. C.; Agrawal, K. M.; Verma, P. S.; Bhattacharjee, S. *Energy Fuels* **1989**, *3*, 15–20.
(9) Kessel, D. *Erdöl Erdgas Kohle* **1990**, *106*, 202–205.
(10) McNaughton, J. L.; Mortimer, C. T. *Int. Rev. Sci., Phys. Chem. Ser. II* **1975**, *10*, 1.
(11) Wesolowski, M. *Thermochim. Acta* **1981**, 21–45.
(12) Flaherty, B. *J. Appl. Chem. Biotechnol.* **1971**, *21*, 144–148.
(13) Faust, H. R. *Thermochim. Acta* **1978**, *26*, 383–398.
(14) Miller, R.; Dawson, G. *Thermochim. Acta* **1980**, *41*, 93–105.
(15) Handoo, J.; Srivastava, S. P.; Agrawal, K. M.; Joshi, G. C. *Fuel* **1989**, *68*, 1346–1348.
(16) Claudy, P.; Létoffé, J.-M.; Chagué, B.; Orrit, J. *Fuel* **1988**, *67*, 58–61.
(17) Schuster, D. S.; Magill, J. H. *Polym. Mater. Sci. Eng.* **1989**, *61*, 242–246.
(18) Nöel, F. *Thermochim. Acta* **1972**, *4*, 377–392.
(19) Giavarini, C.; Pochetti, F. *J. Therm. Anal.* **1973**, *5*, 83–94.
(20) Moynihan, C. T.; Shahriari, M. R.; Bardacki, T. *Thermochim. Acta* **1982**, *52*, 131–141.
(21) Yasufuku, S. *J. Jpn. Pet. Inst.* **1984**, *27*, 525–532.
(22) Crine, J.-P.; Duval, M.; St-Onge, H. *IEEE Trans. Electr. Insul.* **1985**, *EI-20*, 419–422.
(23) Redelius, P. *Thermochim. Acta* **1985**, *85*, 327–330.
(24) Abou El Naga, H. H.; Salem, A. E.; Abd El Ghaffar, D. A. *J. Therm. Anal.* **1986**, *31*, 21–31.
(25) Claudy, P., Létoffé, J.-M., Neff, B.; Damin, B. *Fuel* **1986**, *65*, 861–864.
(26) Bosselet, F.; Létoffé, J.-M.; Claudy, P. *Thermochim. Acta* **1983**, *70*, 7–18.
(27) Bosselet, F.; Létoffé, J.-M.; Claudy, P. *Thermochim. Acta* **1983**, *70*, 19–34.
(28) Bosselet, F.; Létoffé, J.-M.; Claudy, P. *Thermochim. Acta* **1983**, *70*, 35–47.
(29) Bosselet, F.; Létoffé, J.-M.; Claudy, P. *Thermochim. Acta* **1983**, *70*, 49–62.

Table I. DSC Measurements on *n*-Alkane Calibration Standards

| standard (alkane) | lit. values | | DSC measurements | | | | | |
|---|---|---|---|---|---|---|---|---|
| | mp, °C | $\Delta H_f$, cal/g | gradient, °C/min | range, °C | onset, °C | $\Delta H_f$, cal/g | $\Delta T$,[c] °C | $\Delta(\Delta H_f)$,[c] cal/g |
| | | | −10 | +80 to −145 | −87.0 | 26.4 | | |
| $n$-$C_7$ | −90.56[a] | 33.5[a] | +10 | −145 to +40 | −85.0 | 34.1 | −5.6 | −0.6 |
| | | | −10 | +80 to −110 | −23.2 | 46.9 | | |
| $n$-$C_{10}$ | −29.66[a] | 48.3 | +10 | −145 to +60 | −21.6 | 46.5 | −8.1 | +1.8 |
| | | | −10 | +80 to −20 | −3.8 | 51.2 | | |
| $n$-$C_{12}$ | −9.65[a] | 51.8[a] | +10 | −145 to +85 | −3.7 | 51.7 | −6.0 | +0.1 |
| | | | −10 | +80 to −110 | +33.9 | 58.0 | | |
| $n$-$C_{18}$ | +28.24[b] | 57.7[b] | +10 | −145 to +60 | +34.0 | 58.7 | −5.8 | −1.0 |
| | | | | | | mean[d] | −6.4 | +0.1 |

[a] Finke, H. L.; Gross, M. E.; Waddington, G.; Huffman, H. M. *J. Am. Chem. Soc.* **1954**, *76*, 333–341. [b] Schaerer, A. A.; Busso, C. J.; Smith, A. E.; Skinner, L. B. *J. Am. Chem. Soc.* **1955**, *77*, 2017–2018. [c] Difference between literature value and measured values. [d] Mean values for all four standards.

of the instrument were adjusted before the procedure was repeated. In the present case, where low-temperature analyses were required, a series of pure (>99%) *n*-alkanes whose melting points covered the temperature range of interest were used for an additional low-temperature correction. The standards were analyzed using the same temperature program as for the oil samples. As only melting points and melting enthalpies are known for *n*-alkanes, the instrument could be property calibrated only during heating scans. Ideally, observed extrapolated onset temperatures should be corrected for any deviation in the angle of the tangent to the "leading edge" from that of the In standard; on the average this correction turned out to be of no significance. From Table I it can be seen that the overall correction of the temperature scale using a +10 °C/min temperature gradient is −6 °C and that no correction of the energy scale is needed. By recording the melting point of *n*-octadecane ($n$-$C_{18}$) using different temperature gradients and extrapolating to zero (i.e., isothermal programming), it was found that the temperature offsets caused by temperature programming were only marginal for both + 10 and −10 °C/min gradients; hence it was concluded that a −6 °C correction of the temperature scale provided an adequate adjustment of the instrument readings in both cooling and heating scans. Recommendations for temperature[30-32] and heat flow[33] calibrations of DSC instruments have been given recently.

**Data Processing.** Sample thermograms were obtained by subtracting the baseline from the raw thermogram. Furthermore, to determine the heat flow of the thermal processes involved during the temperature scan, a *processing* baseline had to be defined (Figure 2). In the case of heating scans the baseline was determined by the ending of the glass transition and the ending of the endothermal "peak" (end of wax dissolution). In cooling scans processing baselines were similarly determined by the beginning of the exothermal "peak" (onset of wax precipitation) and the beginning of the glass transition. The TADS software has a built-in routine for calculating the total area (energy) of peaks defined by the processing baseline and the thermogram; areas are expressed as calories per gram on the basis of the total heat flow (mcal/s), the total scan time (s) and the amount of sample (g). Besides, there is a routine for determining the glass transition temperature defined as the inflection point (*midpoint*) of the transition. An additional special routine provides for partial areas calculations and enables the listing and plotting of cumulated area versus temperature. Several recommendations on thermal analyses by DSC have been given recently.[34-37]

## Results and Discussion

Seventeen North Sea crude oils of varying composition and paraffinicity, in the following consecutively numbered 1–17, have been analyzed by DSC. These are the same oils that have been further analyzed in parts 1[1] and 2[2] of this series of papers. The results of the DSC analyses in the temperature range of +60 to −140 °C are shown graphically in Figure 1a–c by representative thermograms for all 17 oils; the designations a, b, and c refer to the different types of oils encountered, i.e., condensates/light oils, paraffinic oils, and waxy/biodegraded oils, respectively. Figure 2 shows an enlarged set of typical thermograms illustrating the most important features common to all oils, i.e., the broad endothermal/exothermal peaks, the processing baselines, the glass transitions, and the onset and end-point temperatures. For oils 4, 6, (7), 8, 9, 12, 13, and 15, a sharper endothermal peak (spike) separated from the main endotherm is also visible. This peak is supposed to arise from the melting of *n*-alkanes with a relatively narrow melting range.[13] For some of these oils, 4, 12, 13, and 15, a similar exothermal peak is also present. These oils are relatively light (oils 4, 12, and 13 are condensates) and mainly paraffinic in nature. The presence of such a peak also resembles what was recently observed in waxes with a high ratio of macrocrystalline to microcrystalline material.[38] Hence it may be concluded that these peaks are associated with the thermal transitions (liquid–solid and vice versa) of macrocrystalline wax consisting of mainly *n*-paraffins, while the remaining shallow but broader peak of the thermogram is due to the more complicated thermal transitions of the crystalline–amorphous wax phases including solid–solid transitions, e.g., orthorhombic-hexagonal transitions as described for the intermediate *n*-paraffin range ($C_{20}$–$C_{40}$).[39]

**Wax Precipitation Temperature (WPT).** WPT is the temperature at which the first wax crystals appear upon cooling of an oil as an effect of the decreased solvating capacity of the oil matrix; this temperature may be compared with the cloud point obtained under standardized conditions.[40] Several authors have observed good correlations between cloud points and WPTs determined by DSC.[18,22,24,25] In DSC analyses WPT is defined as the onset temperature of the exothermal peak. The built-in routine determines the beginning of peaks by their extrapolated onset temperatures defined as the intersection of the inflection line of the peak front (leading edge) with the

(30) ASTM E 967-83 (1987). *Annu. Book ASTM Stand.* **1990**, *14.02*, 595–598.
(31) Höhne, G. W. H.; Cammenga, H. K.; Eysel, W.; Gmelin, E.; Hemminger, W. *Thermochim. Acta* **1990**, *160*, 1–12.
(32) Menczel, J. D.; Leslie, T. M. *Thermochim. Acta* **1990**, *166*, 309–317.
(33) ASTM E 968-83 (1987). *Annu. Book ASTM Stand.* **1990**, *14.02*, 599–602.
(34) Callanan, J. E.; Sullivan, S. A. *Rev. Sci. Instrum.* **1986**, *57*, 2584–2592.
(35) ASTM D 4419-84. *Annu. Book ASTM Stand.* **1990**, *14.03*, 529–532.
(36) ASTM E 793-85 (1989). *Annu. Book ASTM Stand.* **1990**, *14.02*, 518–520.
(37) ASTM E 794-85 (1989). *Annu. Book ASTM Stand.* **1990**, *14.02*, 521–523.
(38) Stank, J.; Mullay, J. *Thermochim. Acta* **1986**, *105*, 9–17.
(39) Turner, W. R. *Ind. Eng. Chem. PRD* **1971**, *10*, 238–260.
(40) ASTM D 2500-88. *Annu. Book ASTM Stand.* **1990**, *05.02*, 201–203.

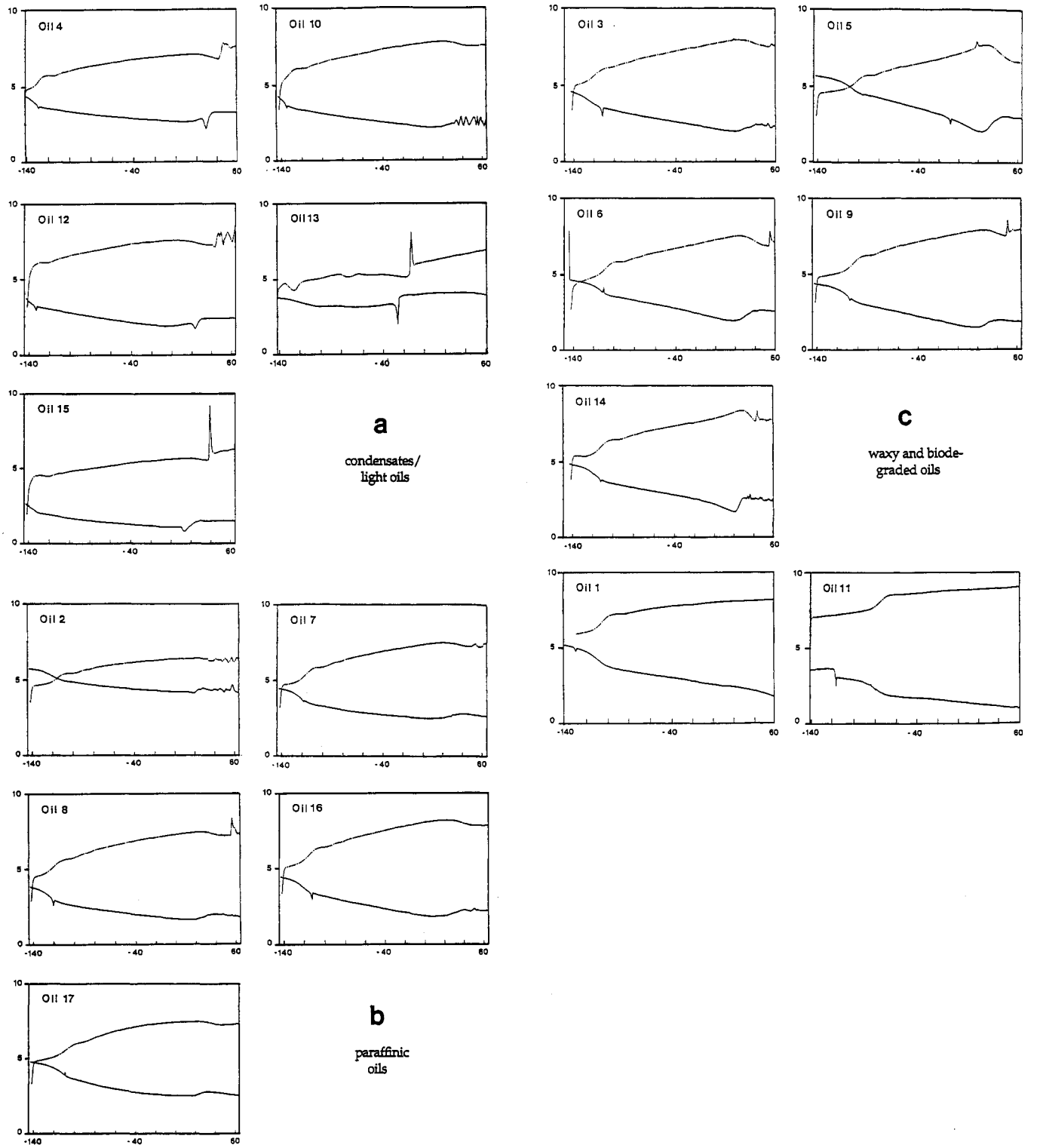


**Figure 1.** DSC measurements on different types of crude oils: (a) condensates/light oils; (b) paraffinic oils; (c) waxy and biodegraded oils. Lower curve: scans from +60 to −140 °C at −10 °C/min, upper curve: scans from −140 to +60 °C at +10 °C/min.

processing baseline. However, as crude oil thermograms often have irregular leading edges, the automatic peak detection routine may give unreliable results. It was therefore decided to determine WPTs manually and directly from the thermograms as the point where the deviation of the exothermal peak from baseline first became visible. The overall standard deviation of these determinations is about 2 °C, and the results corrected for instrument offset (−6 °C) are listed in Table II. Values range from −26.0 °C for the very light condensate (oil 13) to +39.5 °C for oils with a relatively high wax content (oils 5 and 6). These values fall within the same range as those determined recently for another series of crude oils.[16] Based on the measured WPTs, the oils may be grouped as follows: oil 13 (−26 °C), oils 1 and 2 (11–17 °C), oils 12, 14, 15, and 17 (21–26 °C), oils 3, 4, 7, 8, 9, 10, and 16 (32–34 °C), and finally oils 5 and 6 (40 °C).

In part 1 the observed WPTs from DSC were compared with the equivalent temperatures determined by microscopy and viscometry.[1] On the average, WPTs determined by DSC were about 8 °C lower than those determined by microscopy, while the DSC and viscometry data were comparable; however, there was a considerable scatter in the data. The higher WPTs determined by microscopy

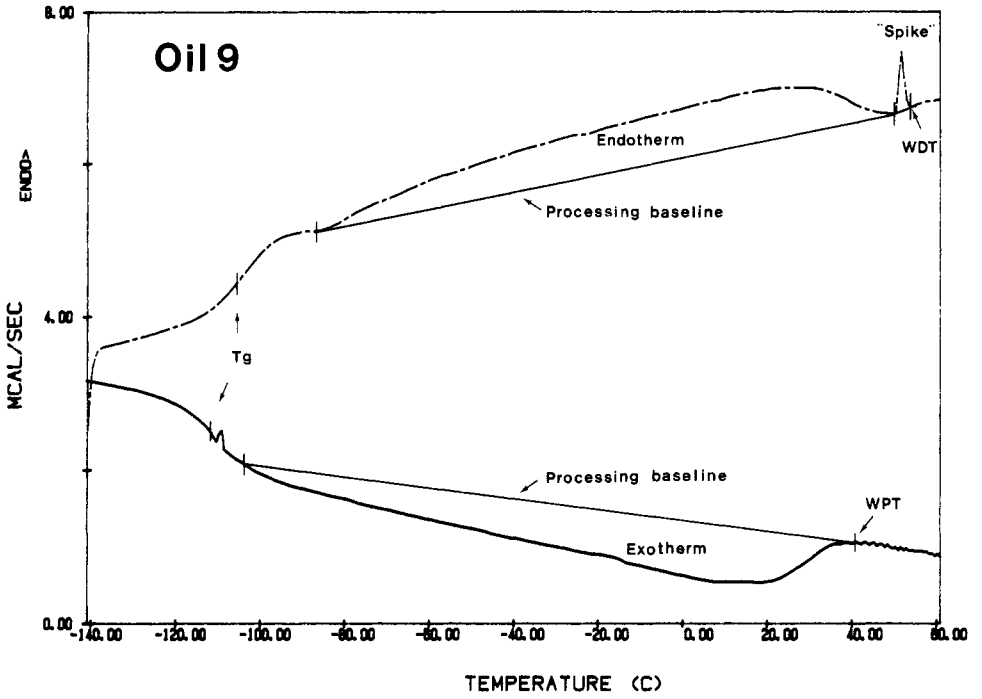


**Figure 2.** Typical DSC thermograms of a crude oil showing the *processing baselines*, $T_g$, WDT, WPT, and a *spike*; lower curve, exotherm; upper curve, endotherm.

**Table II. DSC Measurements on Crude Oils**[a]

| | temperatures[f] | | | enthalpies[f] | |
|---|---|---|---|---|---|
| oil no. | $T_g$,[b] °C | WPT, °C | WDT, °C | $\Delta H_{wpo}$,[c] cal/g | $\Delta H_{wdo}$,[c] cal/g |
| 1 | -110.5 | 11.0 | 37.0 | 0.55 | 1.85 |
| 2 | -115.0 | 17.0 | 30.5 | 4.16 | 6.52 |
| 3 | -118.5 | 33.5 | 40.0 | 5.92 | 6.85 |
| 4 | -128.5 | 32.5 | 46.5 | 9.79 | 9.38 |
| 5 | -103.0 | 39.5 | 53.5 | 9.08 | 10.63 |
| 6 | -107.5 | 39.5 | 46.5 | 8.01 | 9.09 |
| 7 | -116.5 | 32.0 | 47.0 | 4.95 | 7.03 |
| 8 | -119.0 | 32.0 | 53.0 | 5.91 | 8.05 |
| 9 | -104.0 | 31.5 | 48.5 | 5.54 | 6.33 |
| 10 | *d* | 31.5 | 40.0 | 6.34 | 8.27 |
| 11 | -81.5 | nm[e] | 34.0 | nm | 0.32 |
| 12 | *d* | 25.5 | 37.5 | 8.12 | 8.23 |
| 13 | *d* | -26.0 | -16.0 | 7.76 | 6.77 |
| 14 | -112.0 | 23.0 | 40.5 | 5.76 | 6.55 |
| 15 | *d* | 20.5 | 35.5 | 6.63 | 4.97 |
| 16 | -115.0 | 34.0 | 43.5 | 6.62 | 6.98 |
| 17 | -109.0 | 24.0 | 39.0 | 5.51 | 6.67 |

[a] The oils have the following characteristics:[1] Condensates/light oils: 4, 10, 12, 13, and 15. Paraffinic oils: 2, 7, 8, 16, and 17. Waxy oils: 3, 5, 6, 9, and 14. Biodegraded oils: 1 and 11. [b] Measured during heating scans. [c] Calories per gram of total sample. [d] $T_g$ below -130 °C. [e] nm = not measurable. [f] Mean values of up to five measurements.

are probably caused by the higher sensitivity of this instrument; i.e., the nucleation and growing of wax crystals are visible in the microscope before the equivalent concentration has increased sufficiently to be detectable by DSC. As has been observed previously,[18,41] WPTs increase with increasing wax content, in particular with increasing *n*-paraffin content.[22] For crude oil distillates,[16] WPTs were observed to correlate with the upper boiling limit (i.e., highest *n*-alkane) of the fractions. However, not only wax content but also the composition of wax and crude oil per se, i.e., range of *n*-paraffins, content of isoparaffins, naphthenes, asphaltenes, etc., influence the solubility of wax and hence WPT.

**Wax Dissolution Temperature (WDT).** WDT is the temperature at which all precipitated wax has been dissolved upon heating the oil. As for WPTs, the WDTs were determined manually and directly from the thermograms as the endpoint of the endothermic peak (i.e., return to baseline); there is no built-in routine for determining extrapolated peak endpoint temperatures in analogy with the extrapolated onsets. Replicate measurements gave an overall standard deviation of about 2 °C. The results fell in the range of -16.0 °C (oil 13) to 53.5 °C (oil 5), Table II. The dissolution temperatures have also been compared with the results obtained by microscopy.[1] As for WPTs, the WDT data from microscopy are higher than those from DSC, 5 °C on the average. Again this is probably due to the greater sensitivity of microscopy. Comparing the WPT and WDT data one finds that the WDTs are higher than the WPTs by 13 °C on the average; this is probably caused by undercooling/overheating phenomena arising from nonequilibrium conditions during the relatively fast temperature scanning. To avoid this, scan rates approaching zero should be applied, which, however, would give reduced sensitivity as the DSC signal is the time derivative of the heat flow. Also, matrix interferences may play a vital role; this is because nucleation and crystal growth probably respond differently to matrix effects than does dissolution of wax crystals. A similar downward shift of 10–12 °C and 5–8 °C upon cooling has also been observed for lube oils[18] and paraffinic waxes,[13] respectively. Another reason for the relatively large discrepancy between WPTs and WDTs that should not be overlooked stems from the difficulty in defining appropriate processing baselines. Bad signal-to-noise ratios and leading/ending transients of some of the thermograms made it very difficult to determine the processing temperature limits, especially at the high-temperature end.

**Glass Transition Temperature ($T_g$).** Upon continued cooling, that part of the oil matrix which cannot crystallize transforms into a frozen solid (a *glass*) with drastically reduced molecular mobility. This transition, accompanied

(41) Krishna, R.; Bhattarcharjee, S.; Joshi, G. C.; Singh, H.; Purohit, R. C.; Dilawar, S. V. K.; Singh, K. K. *Erdöl Kohle Erdgas Petrochem.* **1989**, *42*, 72–75.

by a rapid increase in viscosity and decrease in heat capacity, is called the *glass transition*, and its midpoint is defined as $T_g$. Below $T_g$ a glassy and a crystalline phase can exist, while above $T_g$ a crystalline and a liquid phase is possible. The DSC analyses have been extended beyond the glass transition of the crude oil matrices. As $T_g$s in heating scans were more easily determined, only these values are given in Table II. $T_g$ was determined as the midpoint of the transition defined by the inflection point. For the 17 oils studied, the observed values fell within the temperature range of −128.5 °C for oil 4 to −81.5 °C for oil 11. For four of the oils, however, namely oils 10, 12, 13, and 15, the glass transition occurred at such low temperatures that it was either beyond the scan limit or coincided with a leading apparatus transient, which made it impossible to determine $T_g$. These four oils were all condensates or light oils with a relatively high content of lower *n*-paraffins. Comparing these results with the recent work of Claudy et al.[16] on crude oils and their distillates, it may be concluded that the glass transition is lowered with decreasing boiling range of the oil. A similar observation was made by Nöel,[18] and this relationship is in accordance with what has been observed for *n*-paraffins.[42] Immediately following the glass transition upon heating, a small exotherm was observed with most oils. This observation is similar to that of Nöel[18] and Claudy et al.[16] who concluded that cooling rapidly below the glass transition could partly prevent crystallization due to the drastically reduced molecular mobility of the frozen matrix. On reheating to a temperature above the glass transition, the mobility would increase and an additional exothermal crystallization could take place. The minimum of this exotherm has been defined as the onset of wax dissolution and hence the beginning of the processing baseline. By this definition, the onset of wax dissolution for all the oils studied is comparable to the glass transition, and onset temperatures ranging from −132 °C (oil 13) to −69 °C (oil 11) were observed (Figure 1a–c). Based on these onset temperatures, a grouping of the oils in accordance with their general characteristics seemed possible: condensates/light oils, oils 13, 12, 15, 10, and 4 (−132 to −120 °C), paraffinic oils, oils 8, 7, 2, and 16 (−108 to −105 °C), and waxy oils, oils 14, 6, 9, and 5 together with the biodegraded oil, oil 1 (−100 to −91 °C) and the heavy biodegraded oil, oil 11 (−69 °C). From this it seemed evident that oil 11 was more severely biodegraded than oil 1, in agreement with GC analysis. Besides, this grouping based on onset temperatures follows almost exactly the same order as that according to the amount of $C_{10+}$ fraction (cf. Table II in part 1).[1] Hence it may concluded that the content of very low molecular weight compounds ($<C_{10}$) plays a major role in determining the glass transition and onset of wax dissolution. A similar grouping based on WDT or WPT data was not observed, and distinctly different properties are probably responsible for the beginning and ending of the wax dissolution and precipitation processes, respectively; this is in accordance with previous observations which have shown that $T_g$ was not influenced by wax content.[18]

**Wax Precipitation Enthalpy ($\Delta H_{wpo}$).** DSC analyses of crude oils reveal heat flows connected to thermodynamic processes taking place during heating or cooling, e.g., precipitation or dissolution of solid matter (wax). The representative thermograms in Figure 1a–c for each of the 17 oils studied show the resulting shallow broad cooling exotherms ranging from about +40 to about −100 °C beyond which the glass transition follows. The total energy released during cooling is proportional to the area enclosed by the exotherm and the processing baseline as shown in Figure 2. As mentioned previously, oils 4, 12, 13, and 15 also gave a leading peak in front of the broad exotherm. Table II lists the measured enthalpies expressed as calories per gram of sample; all values are averages of generally five measurements of each sample. The overall standard deviation was 0.3 cal/g of oil. As enthalpies calculated on the basis of the actual amount of wax involved are not directly accessible from the DSC data, a distinction is made between enthalpies based on the total amount of oil ($\Delta H_{wpo}$) and the actual amount of wax ($\Delta H_{wpw}$, Table III). Values of $\Delta H_{wpo}$ range from 0.55 to 9.79 cal/g of oil for oils 1 and 4, respectively; no values were obtained for oil 11 (heavily biodegraded). Differences in enthalpies between oils probably reflect their varying composition and content of precipitable matter (wax), although grouping of the oils in accordance with the general classification (i.e., paraffinic, waxy etc.) did not correlate with the observed enthalpies. However, plotting of $\Delta H_{wpo}$ versus the $C_{20+}$ or the $C_{30+}$ amount (cf. part 4, supplementary material)[3] revealed a good correlation for most oils as enthalpies increased with increasing $C_{20+}$ or $C_{30+}$ content; the light oils 4, 10, 12, and 15 plotted well above the regression line, while oil 9 (waxy) fell below. This shows that the condensates/light oils, probably due to their relatively high proportion of lower *n*-alkanes, behave uniquely with respect to wax precipitation. In general, a linear relationship between transition enthalpies and *n*-paraffin content has been observed.[19,21,22] In addition to the enthalpy involved in the liquid–solid transitions, the broad exotherms probably also include the enthalpy involved in intracrystal solid–solid transitions analogous to the transitions described for pure *n*-alkanes.[39] The leading spikes observed for some oils (oils 4, 12, 13, and 15) are supposed to originate from the initial crystallization of a limited range of *n*-paraffins at the beginning of the cooling process. This conclusion, however, is not supported by HTGC-MS analyses of waxes precipitated from oil 4 at temperatures slightly above ambient (23 and 40 °C) as they revealed a major content of isoparaffins (50% compared to 25% of *n*-alkanes).[1] On the other hand, wax isolated from oil 4 by acetone precipitation at −25 °C (*total wax*) contained up to 70% *n*-paraffins. Besides, the

**Table III. Calculated Average Wax Transition Enthalpies in the Temperature Range from WPT/WDT to −40 °C**

| oil no. | pulsed NMR[a] cool/heat,[b] wt % solid | DSC partial area cool,[c] % | DSC partial area heat,[d] % | | enthalpies $\Delta H_{wpw}$,[e] cal/g | enthalpies $\Delta H_{wdw}$,[e] cal/g |
|---|---|---|---|---|---|---|
| cond/light | | | | | | |
| 4 | 8.5 | 60.5 | 56.7 | | 69.8 | 62.7 |
| 10 | 7.1 | 56.9 | 57.3 | | 50.5 | 67.0 |
| 12 | 5.9 | 51.4 | 51.6 | | 70.6 | 71.7 |
| 15 | 5.4 | 50.2 | 55.8 | | 61.4 | 51.7 |
| | | | | means | **63.1** | **63.3** |
| paraffinic | | | | | | |
| 2 | 7.0 | 57.4 | 56.2 | | 34.4 | 52.2 |
| 7 | 8.3 | 63.3 | 63.2 | | 38.1 | 53.3 |
| 8 | 8.0 | 59.2 | 63.7 | | 43.7 | 64.5 |
| 16 | 10.5 | 63.8 | 67.4 | | 40.1 | 44.9 |
| 17 | 12.7 | 54.8 | 61.2 | | 23.7 | 32.3 |
| | | | | means | **36.0** | **49.4** |
| waxy | | | | | | |
| 3 | 10.5 | 68.1 | 65.1 | | 38.3 | 42.8 |
| 5 | 14.6 | 83.8 | 82.6 | | 52.2 | 60.0 |
| 6 | 12.5 | 78.4 | 75.3 | | 50.2 | 54.8 |
| 9 | 11.6 | 74.4 | 74.0 | | 35.5 | 40.2 |
| 14 | 10.4 | 72.2 | 72.9 | | 40.3 | 46.3 |
| | | | | means | **43.3** | **48.8** |

[a] Cf. part 2, Table III.[2] [b] Average values of equilibrium measurements during cooling and heating. [c] Cooling at −10 °C/min. [d] Heating at +10 °C/min. [e] Calories per gram of wax.

(42) Stearns, R. S.; Duling, I. N.; Johnson, R. H. *Ind. Eng. Chem. Process Res. Dev.* **1966**, *5*, 306–313.

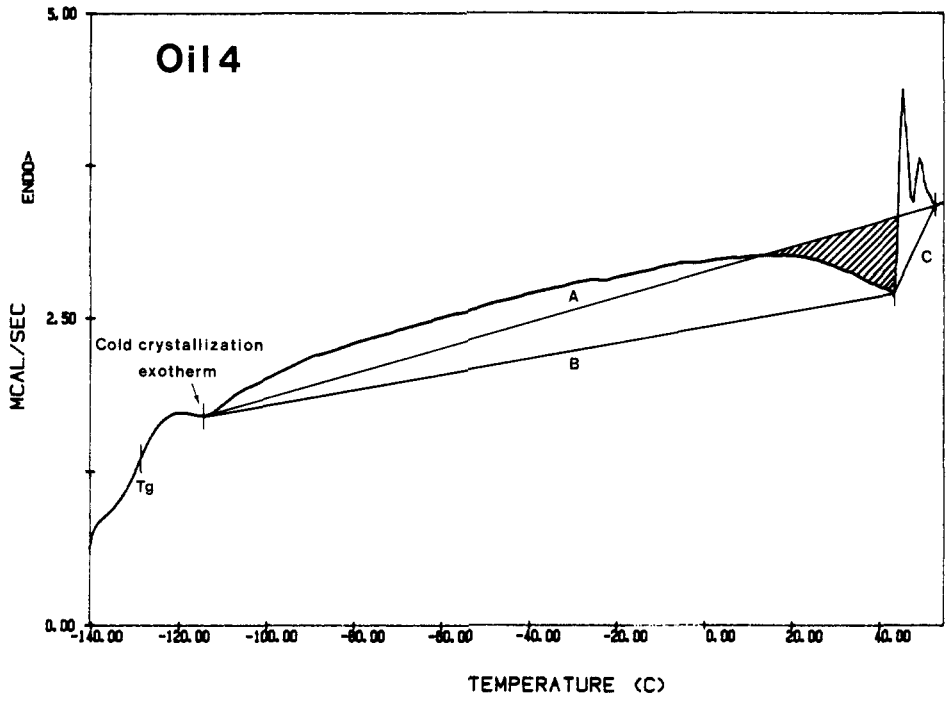


**Figure 3.** DSC endotherm of oil 4 showing the use of either a continuous straight baseline (A) or a discontinuous baseline (B + C).

crystallization of *n*-paraffins is supposed to be distinctly different from the precipitation of the more microcrystalline/amorphous wax-forming material which probably takes place over a much broader temperature range as seen from other studies of waxes.[7,39] In recent studies of the precipitation of wax from middle distillate fuels, the distribution of *n*-paraffins in the precipitate was observed to vary with the initial composition and the precipitation temperature;[43-45] decreasing temperatures shifted the distribution toward the lower carbon numbers, an observation which adds to the general view that the higher the *n*-alkane number, the higher is the precipitation temperature. As observed with *n*-alkanes, cocrystallization and formation of solid solutions or eutectic mixtures also play a significant role in solubility behaviour.[39,46] Hence it must be emphasized that crude oils are very complex systems and that wax precipitation depends not only on temperature, but also on composition, wax content, and natural wax inhibitors, which may inhibit either nucleation or crystallization or both.

**Wax Dissolution Enthalpy ($\Delta H_{wdo}$).** On heating the oil samples from below the glass transition up to 70 °C, broad endotherms were obtained as a result of wax dissolution (Figure 1a–c). Figure 2 shows an example of how the processing baseline is limited by the glass transition at low temperatures and the ending of the endotherm at higher temperatures. Based on the total heat flow within these processing limits, the total enthalpy was calculated. As for the precipitation enthalpies, a distinction was made between values based on total amount of oil ($\Delta H_{wdo}$) and on the actual amount of wax ($\Delta H_{wdw}$, Table III). The average values of the measured $\Delta H_{wdo}$s are listed in Table II for each of the 17 oils studied. The enthalpies range from 1.85 to 10.63 cal/g of oil for oils 1 and 5, respectively. No obvious correlation of dissolution enthalpies with the descriptive terms paraffinic, waxy, etc. was observed.

The measured $\Delta H_{wdo}$s are supposed to be directly proportional to the amount of wax precipitated during a cooling scan and hence should be comparable to the corresponding $\Delta H_{wpo}$s. However, $\Delta H_{wdo}$s are greater than the corresponding $\Delta H_{wpo}$s for all but three oils (oils 4, 13, and 15). The average excess of dissolution enthalpy for all oils is about 0.9 cal/g of oil (~14%). This enthalpy difference could not be accounted for thermodynamically, whereas several other possible explanations could be put forward. First, great uncertainty in the experimental data probably can be ruled out as the observed trend seemed very constant. A second explanation could be that additional crystallization took place during the span of time from the moment the cooling scan terminated till the heating scan began. However, the excess of endothermal enthalpy was not observed to be dependent on this time interval, which it should be with additional crystallization taking place beyond the glass transition. Furthermore, this process would seem fairly unlikely as the molecular mobility below $T_g$ is negligible. However, as has been pointed out previously, additional crystallization probably does take place immediately following the glass transition upon heating. This transition was visible in most oils as a plateau or small exotherm just above the ending of the glass transition (Figure 3). According to Nöel,[18] this small exotherm could be eliminated by annealing the sample, i.e., by subsequent *slow* cooling below this crystallization temperature. Unfortunately, this cold crystallization phenomenon has influenced the enthalpy measurements in two ways: firstly, as not all components did crystallize upon cooling, the precipitation exotherm became too small by an amount corresponding to the area of the small exotherm, and secondly, as the endotherm processing baselines were always drawn from the minimum of this exotherm and not from a supposedly more "real" beginning of the dissolution process as of annealed samples, the dissolution endotherm became too large. Rough estimates showed that these effects could well account for about a 10% difference between precipitation and dissolution enthalpies. However, as none of the oil samples were annealed prior to heating

(43) Affens, W. A.; Hazlett, R. N.; Smith, D. E. NRL Report 8692, Naval Research Laboratory, Washington, DC, 1983; 12 pp.
(44) Affens, W. A., Hall, J. M.; Holt, S.; Hazlett, R. N. *Fuel* **1984**, *63*, 543–547.
(45) Van Winkle, T. L.; Affens, W. A.; Beal, E. J.; Hazlett, R. N.; DeGuzman, J. NRL Report 8869, Naval Research Laboratory, Washington, DC, 1985, 40 pp.
(46) Holder, G. A.; Winkler, J. *J. Inst. Petr.* **1965**, *51*, 228–252.

scans, no indications of where the real dissolution process started were obtained, and processing baselines were therefore consistently drawn from the minimum of the small cold crystallization exotherm.

A somewhat similar phenomenon was observed for some of the oils having an ending spike (i.e. oils 4, 6, 7, 8, 9, 12, 13, 14, and 15); just in front of that spike the broad endotherm dived toward a minimum as exemplified by oil 4 in Figure 3. Similar exotherms were observed by Bosselet et al. for $C_{18}$–$C_{25}$ *n*-alkanes in a dewaxed gas oil, and which resulted in lighter ($<C_{20}$) *n*-alkanes having higher enthalpies than the higher ($>C_{20}$) *n*-alkanes. Depending on how the processing baseline was drawn, significantly different enthalpies were obtained. Starting from the exothermal minimum just above the glass transition, a continuous straight baseline (A) resulted in part of the area becoming negative or exothermal (scattered area; −1.14 cal/g of oil), which reduced the final enthalpy to 2.30 cal/g of oil. On the other hand, a discontinuous baseline consisting of one part (B) starting just above the glass transition as for A and ending at the minimum just below the spike giving the area of the broad endotherm (8.55 cal/g) as well as a second part (C) giving the area of the spike (0.72 cal/g) would result in a different total enthalpy of 9.27 cal/g of oil. The latter value is in much closer agreement with the corresponding $\Delta H_{wpo}$ (9.43 cal/g of oil). The exotherm, if the observed minimum is connected to such a process, is typically observed at about 35–45 °C in most oils, and hence probably did not arrive from additional crystallization; it is much more likely due to solid–solid transformations in the crystalline part of the wax. Such transformations have been observed for *n*-alkanes just prior to fusion.[39] The observed spikes then most likely arrived from the dissolution of a limited range of *n*-paraffins, as discussed above. The events were also most outstanding in the condensates/light oils having a relatively high *n*-paraffin content (oils 4, 13, and 15). However, this arises a serious question on how to draw the processing baseline for these oils. A continuous baseline as for the remaining oils would seem obvious, but as we do not have sufficient experimental evidence in support of the transition exotherm concept at present, data have been processed using discontinuous baselines (i.e., B + C). Besides, total dissolution enthalpies based on discontinuous baselines are in much closer agreement with the corresponding precipitation enthalpies than are those based on continuous baselines.

**Calculation of $\Delta H_{wpw}$ and $\Delta H_{wdw}$ Enthalpies by Combining DSC and Pulsed NMR Data.** Thermodynamic models based on regular solution theory for describing wax precipitation from crude oils require the input of wax transition enthalpies (ideally, $\Delta H_f$) as discussed by others.[47-51] However, the experimentally determined enthalpy data presented in this paper (Table II) were not expressed in terms of the actual wax amount but the total sample amount (oil), as the actual amount of wax being precipitated/dissolved during the DSC experiments could not be obtained directly. We therefore also had to study the actual amount of wax (percentage of the whole sample weight) being precipitated as a function of temperature for each oil by means of pulsed NMR (part 2). As no definite discrepancy was observed in the precipitated solids content between cooling and heating experiments, only one set of data (mean values) was presented.[2] By the combination of DSC and corresponding pulsed NMR data (% solid) it was considered possible to express the observed enthalpies in terms of the actual amount of wax present. Pulsed NMR data were obtained in the temperature range from +45 (all wax dissolved) to −40 °C, and by using the partial area routine of the TADS software, corresponding accumulated enthalpies of the same temperature interval (i.e., from WPT/WDT to −40 °C) were extracted from the acquired DSC data. For each oil, that thermogram whose enthalpy was closest to the average value (Table II) was used for calculating the enthalpies presented in Table III. The accumulated DSC area or enthalpy (cal/g of oil) of the temperature interval was multiplied by the total sample amount (g of oil) and divided by the amount of precipitate (g of wax) at −40 °C as determined by pulsed NMR. Enthalpies calculated this way become the *average* values of wax transition enthalpies of this particular temperature range and do not reflect the temperature dependency of the enthalpy. Precipitation enthalpies ($\Delta H_{wpw}$) range from 23.7 to 70.6 cal/g of wax for oils 17 and 12, respectively. For the dissolution enthalpy data ($\Delta H_{wdw}$), the corresponding values are 32.3 to 71.7 cal/g of wax. From Table III it can be seen that the calculated enthalpies are considerably higher for condensates than for paraffinic and waxy oils. For all but two oils, 4 and 15 (condensates), precipitation enthalpies are lower than the corresponding dissolution enthalpies, as described previously. The differences between precipitation and dissolution enthalpies probably reflect the oils' varying composition and their differing tendencies to undergo additional crystallization/transition upon heating. The calculated values are comparable to heats of fusion of pure *n*-alkanes[52] of the intermediate paraffin range ($C_{15}$–$C_{40}$), commercial waxes,[12] and wax precipitated from crude oils.[17]

**Temperature Dependency of Wax Precipitation ($\Delta H_{wp}$) and Dissolution ($\Delta H_{wd}$) Enthalpies.** As wax-forming species can have significantly different heats of fusion and melting points depending on their chemical structure and molecular weight, they tend to precipitate/dissolve at different temperatures; hence, the transition enthalpies, $\Delta H_{wp}$ and $\Delta H_{wd}$, must inherently be temperature dependent. This was discussed recently by Bosselet et al.[27] who used *n*-alkane model systems to evaluate the temperature dependency of wax crystallization enthalpies. They found a reversed parabolic correlation with a maximum of about 50 cal/g of wax at ca. −10 °C. Claudy et al.,[25] however, in a study of diesel fuels, found crystallization enthalpies being linear dependent on temperature. Again by combining pulsed NMR and DSC experimental data, we were also able to determine the temperature dependency of wax precipitation and dissolution enthalpies. The amount of wax was measured at 5 °C intervals from +45 to −40 °C by pulsed NMR with the value at each successive temperature being a measure of the accumulated amount (wt %) of precipitated wax at that temperature. Similarly, from DSC the enthalpy (area) could be accumulated successively at 5 °C intervals from WPT/WDT down to −40 °C. For each temperature, $T'$, the average enthalpy of the temperature range from WPT/WDT to $T'$ was calculated by the partial area routine. Due to some scattering of the pulsed NMR data, especially at low wax concentration, both sets of data were subjected to polynomial curve fitting which smoothed some of the data. Then the partial accumulated enthalpy

(47) Reddy, S. R. *Fuel* **1986**, *65*, 1647–1652.
(48) Won, K. W. *Fluid Phase Equilib.* **1986**, *30*, 265–279.
(49) Won, K. W. *Fluid Phase Equilib.* **1989**, *53*, 377–396.
(50) Majeed, A.; Bringedal, B.; Øverå, S. *Oil Gas J.* **1990**, *June 18*, 63–69.
(51) Chung, F.; Sarathi, P.; Jones, R. *NIPER-498*; National Institute of Petroleum Energy Research, Bartlesville, OK, 1991, 45 pp.
(52) Broadhurst, M. G. *J. Res. NBS* **1962**, *66A*, 241–249.

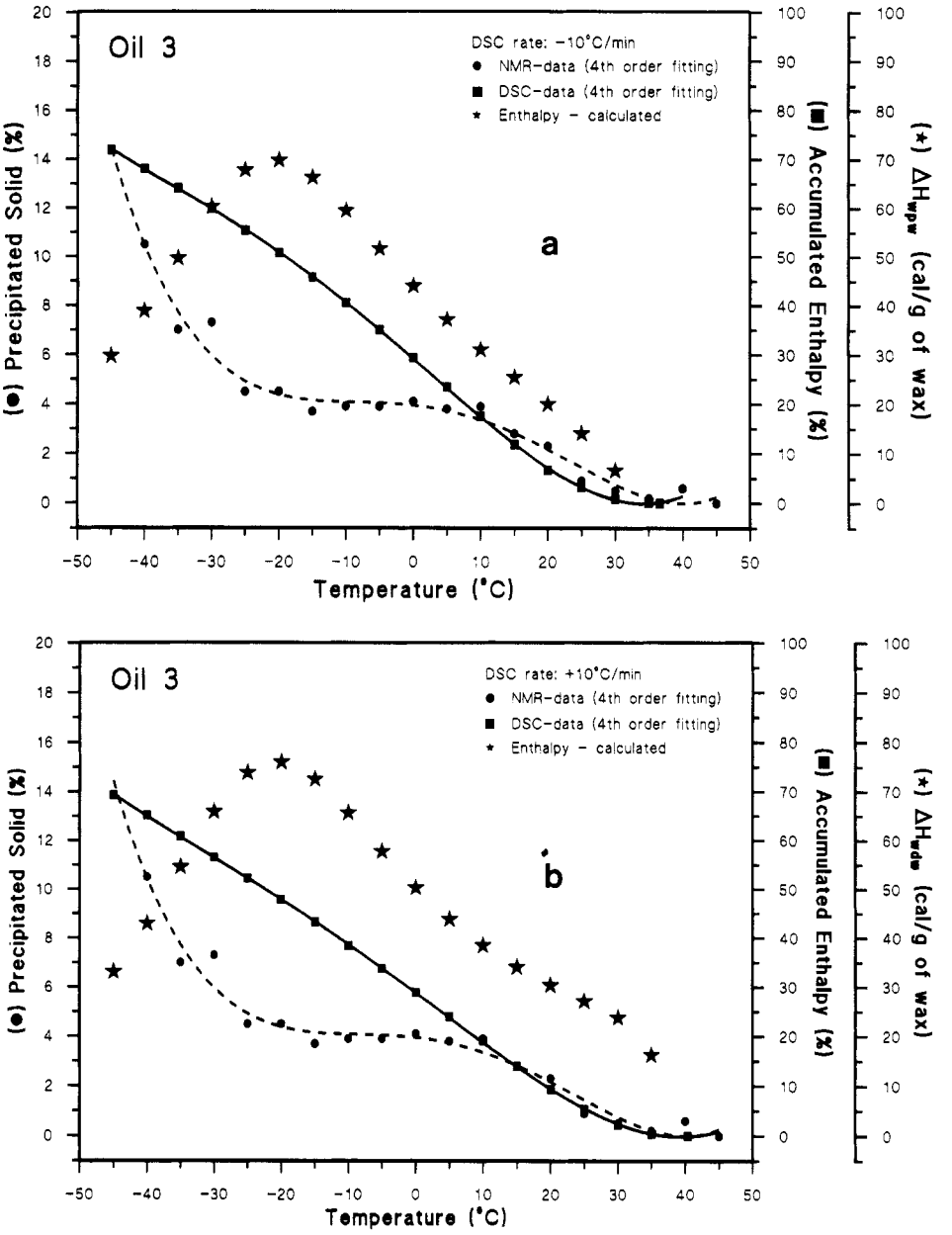


**Figure 4.** Correlation of pulsed NMR and DSC experimental data for oil 3: (a) DSC at −10 °C/min; (b) DSC at +10 °C/min. (●) Pulsed-NMR data (% solid); (■) accumulated DSC enthalpy (%); (★) calculated wax transition enthalpy (cal/g of wax).

polynomial (DSC) was divided by the accumulated amount of wax polynomial (pulsed NMR) and finally multiplied by the total enthalpy (cal/g of oil) to give an *average* wax enthalpy (cal/g of wax) at each successive temperature (5 °C intervals). Figure 4a,b shows an example (oil 3) of the result of these calculations as function of temperature for $\Delta H_{wpw}$ and $\Delta H_{wdw}$, respectively. In both cases the correlation with temperature was found to be parabolic in nature with a maximum about 70 cal/g of wax ($\Delta H_{wdw}$ being higher) at ca. −20 °C, in reasonable accordance with the results of Bosselet et al.[27] This trend is somewhat surprising as one might expect a steady decrease in enthalpy with decreasing freezing temperature as is known from *n*-alkanes.[51] However, according to the HTGC-MS analysis of wax precipitated from oil 4 at different temperatures, it was observed that wax formed at higher temperatures (about 40 °C) consisted primarily of high molecular weight isoparaffins and condensed naphthenes, while the *n*-paraffins did not become dominant until at somewhat lower temperature.[1] Hence, as isoparaffins and naphthenes have lower heats of fusion than *n*-paraffins, the wax transition enthalpies should at first increase with decreasing temperature until a maximum is reached corresponding to maximum *n*-paraffin precipitation; at still lower temperatures, where compounds with lower heats of fusion would precipitate, the enthalpy should again decrease in accordance with the observations. As the order of precipitation is not necessarily the same as that of dissolution, this may also explain the difference between $\Delta H_{wpw}$ and $\Delta H_{wdw}$ and why the spikes mentioned earlier are more rarely observed during cooling scans. However, as a reversed parabolic trend of the temperature dependency was also observed by Bosselet et al.[27] in DSC studies of *n*-alkanes in dewaxed gas oils, the explanation above is incomplete; other processes must also be included, e.g., solid–solid transitions in the initially formed precipitate (wax). Such transitions would have the effect of increasing the enthalpy with decreasing temperature up to the observed maximum, after which the enthalpy again would decrease, as only lower molecular weight compounds with low heats of fusion would be left to precipitate on continued cooling. Additional energy requirements for sol-

id–solid transitions could also account for the reversed parabolic shape of the dissolution enthalpy–temperature relationship.

In principle, the temperature dependency of wax transition enthalpies can be calculated as described above for all oils. In some cases, however, the reversed parabolic trend was not as regular as shown in Figure 4a,b, just as maximum enthalpy values occasionally came out unrealistically high (>100 cal/g of wax) and with doubtful physical meaning. Obviously, the correlation between the pulsed NMR and DSC experimental data is not always straightforward. As discussed in part 2,[2] one problem possibly is related to the determination of solid wax by pulsed NMR. Experiments performed with macrocrystalline (paraffinic) and microcrystalline/amorphous (isoparaffinic/naphthenic) wax fractions seemed to indicate different pulsed NMR response factors for the two types of wax. This raises some fundamental questions on how to interpret and obtain more reliable correlations between the DSC and pulsed NMR experimental data. To clarify this problem further, measurements on different kinds of wax are needed. At present, we have not fully resolved this problem and hence do not wish to elaborate further on the temperature dependency of the precipitation/dissolution enthalpies of crude oil waxes.

## Summary and Conclusions

The characterization of wax precipitation from a series of North Sea crude oils has been achieved by means of DSC by measuring glass transition, wax precipitation, and wax dissolution temperatures together with the wax precipitation and dissolution transition enthalpies. The glass transition temperatures were not correlated with the wax content but with the concentration of the light components in the oil matrix in accordance with the general physical characteristics of the oils. On the other hand, the wax precipitation and dissolution temperatures were much more closely correlated with the wax content and with the dissolution temperatures on the average being 13 °C higher than the corresponding precipitation temperatures. Generally, the dissolution enthalpies were also higher than the corresponding precipitation enthalpies, a phenomenon probably being related to the additional crystallization and/or solid-solid transitions taking place during heating and hence the definition of processing baselines.

By the combination of experimental DSC data with wax precipitation data obtained from pulsed NMR it was possible to calculate *average* wax transition enthalpies for precipitation and dissolution in the temperature range of +45 to −40 °C. Values obtained were comparable to those reported for *n*-alkanes, commercial hydrocarbon waxes, or other crude oil waxes. Furthermore, by using the temperature dependency on wax precipitation as studied by pulsed NMR in combination with the measured DSC enthalpies it was also possible to derive the temperature dependency on the wax transition enthalpies for the same temperature interval as above. This relationship was found to be approximately reversed parabolic in nature with the maximum close to −20 °C, in accordance with another recent study of *n*-alkanes in dewaxed gas oils. However, for some of the oils studied maximum enthalpy values came out unrealistically high (>100 cal/g), and the combination of DSC with pulsed NMR has to be further elaborated to obtain more reliable results on the temperature dependency of wax transition enthalpies.

**Acknowledgment.** We are grateful to the STATOIL-Group for financing this study and for granting permission to publish this paper. The STATOIL-Group consists of STATOIL Efterforskning og Produktion A/S, GHP Petroleum (Denmark) Inc., Total Marine Danmark, LD Energi A/S, EAC Energy A/S, DENERCO K/S and Dansk Olie og Gas Produktion A/S (DOPAS). We also thank STATOIL a.s., Norway, for providing the crude oil samples for the study. Karen Schou Pedersen and Per Skovborg, Calsep A/S, as participants in the project, are greatly acknowledged for many valuable discussions and suggestions.

## Abbreviations

| | |
|---|---|
| DSC | differential scanning calorimetry |
| mp | melting point |
| HTGC-MS | high-temperature gas chromatography–mass spectrometry |
| NMR | nuclear magnetic resonance |
| PVT | pressure–volume–temperature |
| WDT | wax dissolution temperature |
| WPT | wax precipitation temperature |

## Nomenclature

| | |
|---|---|
| $\Delta H$ | enthalpy difference |
| $C_n$ | carbon number |
| $C_{n+}$ | $C_n$ plus fraction |
| *n* | normal |
| % solid | solid weight percent |
| wt % | weight percent |

*Subscripts*

| | |
|---|---|
| f | fusion |
| g | glass transition |
| wd | wax dissolution |
| wp | wax precipitation |
| wdo | wax dissolution based on oil amount |
| wpo | wax precipitation based on oil amount |
| wdw | wax dissolution based on wax amount |
| wpw | wax precipitation based on wax amount |